**Supplementary Information**

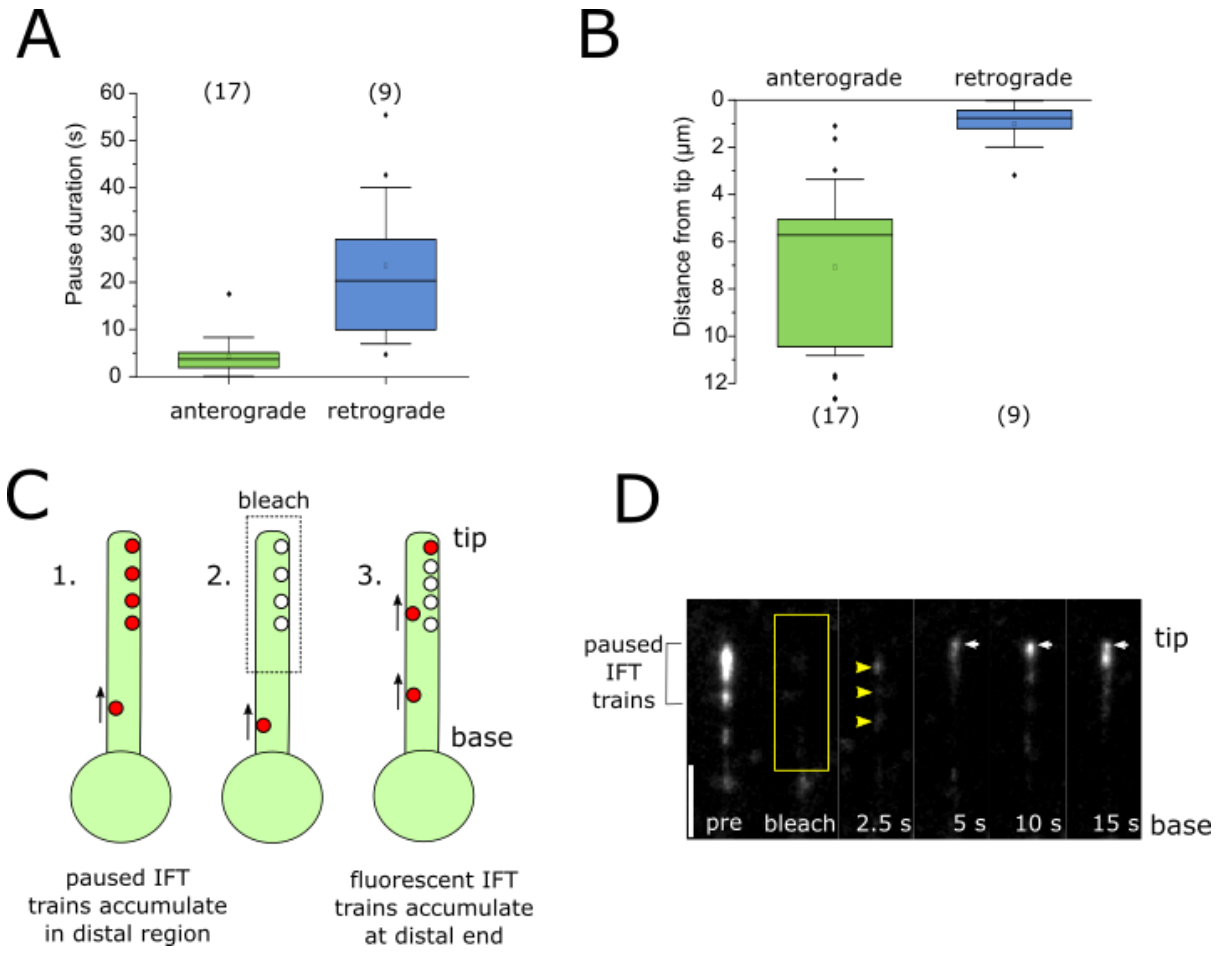


**Figure S1: Accumulation of paused retrograde IFT trains in the distal region of flagella. A)** Box plot showing mean duration of IFT pausing events. n is shown in parentheses. **B)** Box plot showing the position of the IFT train at the onset of pausing. **C**) Schematic representation of FRAP experiment. **D**) Image sequence showing movement of IFT trains following photobleaching of paused IFT trains. After bleaching, the anterograde IFT trains move through the distal region (yellow arrows), before reaching the flagella tip (white arrows).

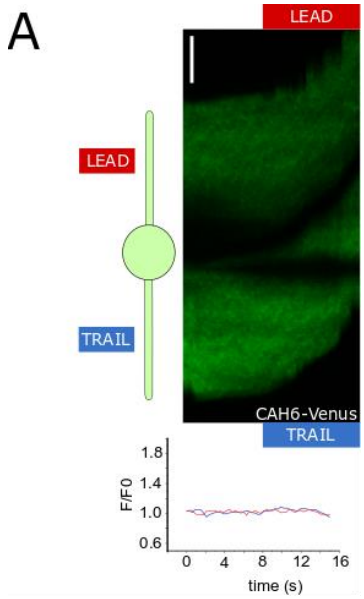


**Fig S2: CAH6-Venus does not show elevations in fluorescence. A**) Kymograph showing gliding movements in cell expressing CAH6-Venus. The graph indicates that no significant changes in fluorescence occur in association with gliding movements (red =lead flagellum, blue = trailing flagellum). Bar = 5 μm.

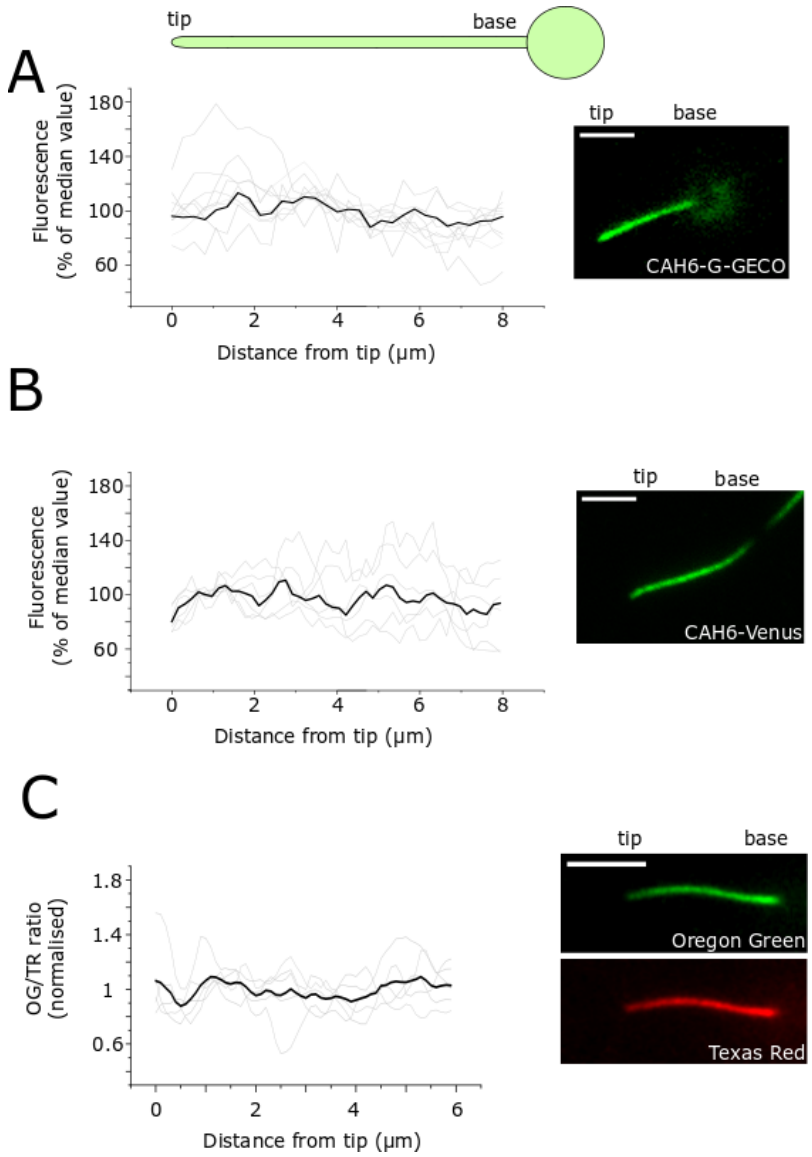


**Figure S3: Resting $[Ca^{2+}]_{fla}$ is uniform along the length of the flagellum. A)** Fluorescence of CAH6-G-GECO along the length of the flagellum. Individual traces (shown in grey) were normalised to the median fluorescence along each flagellum. The median trace is shown in bold. n = 9 flagella. A representative TIRF microscopy image of flagellum expressing CAH6-G-GECO is shown. **B)** Median relative fluorescence of CAH6-Venus along the length of the flagellum. Individual traces (shown in grey) were normalised to the median fluorescence along each flagellum. The median trace is shown in bold. n = 6 flagella. A representative TIRF microscopy image of flagellum expressing CAH6-Venus is shown. **C**) Fluorescence ratio of Oregon Green BAPTA and Texas Red along the length of the flagellum. Individual traces (shown in grey) were normalised to the median fluorescence ratio along the flagellum. n = 5 flagella. TIRF microscopy images of flagellum from a cell biolistically-loaded with Oregon-Green BAPTA dextran (green) and Texas Red dextran (red). Bars = 5 µm.

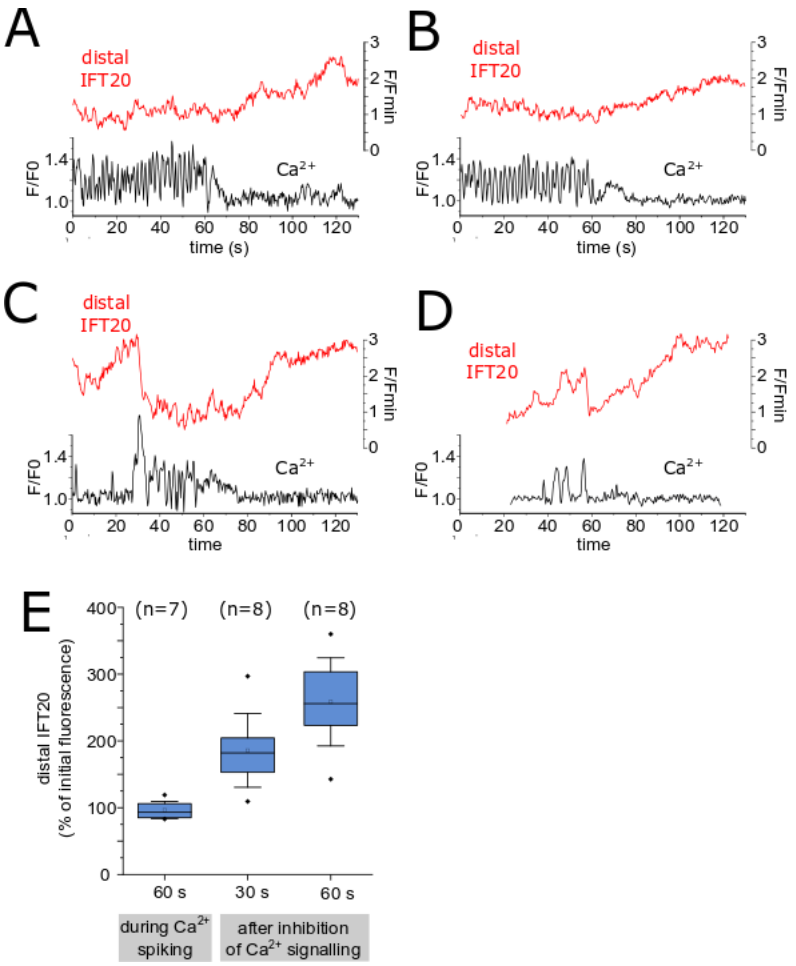


**Figure S4: Inhibition of high frequency $[Ca^{2+}]_{fla}$ elevations. A)** The effect of removing external $Ca^{2+}$ on the accumulation of IFT trains in a flagellum exhibiting high frequency $[Ca^{2+}]_{fla}$ elevations. Simultaneous TIRF imaging of IFT20-mCherry and Oregon Green BAPTA. The cell was initially perfused with a buffer containing 300 µM external $Ca^{2+}$, which was switched to a buffer containing 0 µM $Ca^{2+}$ a t = 0 s. The removal of external $Ca^{2+}$ from the perfusion chamber inhibits $[Ca^{2+}]_{fla}$ elevations after 60 s and leads to accumulation of IFT trains in the distal region of the flagellum (demonstrated by an increase of ITF20-mCherry fluorescence in the distal region - red trace). IFT20-mCherry fluorescence is shown as F/Fmin (Fmin calculated as the lowest mean F over a 10 s period). **B)** A further example of the experiment shown in (A). **C)** As (A), but showing a flagellum exhibiting intermittent $Ca^{2+}$ spiking. **D)** As (A) but showing a flagellum exhibiting low frequency $[Ca^{2+}]_{fla}$ elevations. **E)** Box plots showing IFT20-mCherry fluorescence in the distal region during 60s of $Ca^{2+}$ spiking (mean frequency 0.42 ± 0.03 Hz, SE), or 30 s and 60s after the final $[Ca^{2+}]_{fla}$ elevation was observed. Fluorescence is shown relative to fluorescence at the onset of $Ca^{2+}$ spiking or at time of the final $[Ca^{2+}]_{fla}$ elevation. Box = median and 25-75% confidence interval, mean is open square, error bars represent standard deviation.

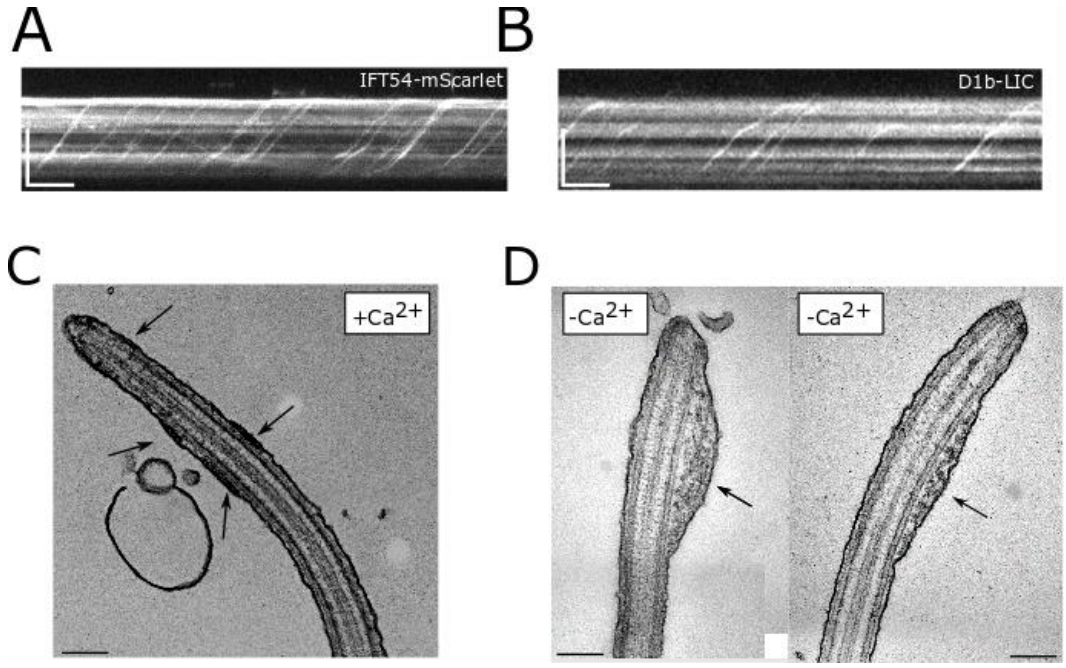


**Figure S5: Inhibiting flagella $Ca^{2+}$ signalling causes large distal accumulations of IFT trains. A)** Kymograph of IFT54-mScarlet after removal of external $Ca^{2+}$ (0 $Ca^{2+}$ buffer + 200 μM EGTA) for 5 minutes. **B**) Kymograph of D1bLIC-GFP after removal of external $Ca^{2+}$ for 5 minutes. Bars = 5 μm and 10 s. **C**) TEM of adherent *Chlamydomonas* flagellum. Transverse section of flagellum indicating the presence of distinct IFT trains (arrowed). Bar = 300 nm. **D**) TEM of transverse sections of adherent flagella following the removal of external $Ca^{2+}$ for 5 minutes. Distinct IFT trains were not observed, but large accumulations of IFT particles (arrowed) can be observed in the distal regions of the flagella (8 out of 8 flagella examined). Bar = 300 nm.

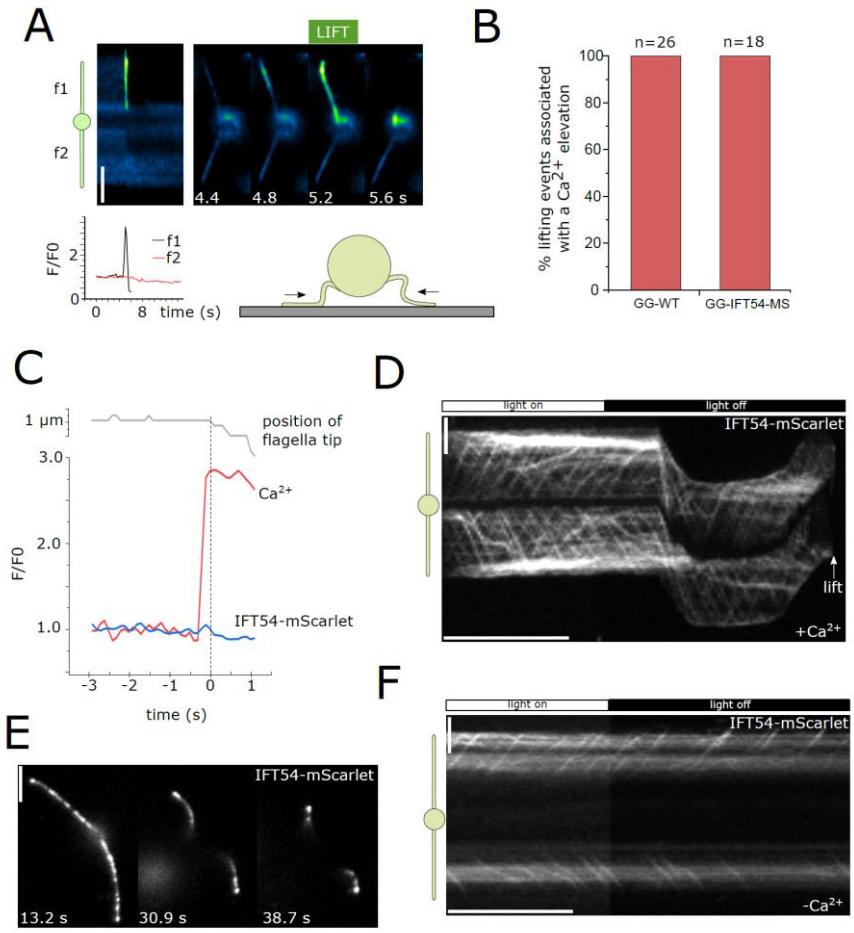


**Figure S6: Flagella lifting is $Ca^{2+}$-dependent. A**) Imaging of $[Ca^{2+}]_{fla}$ elevations during flagella lifting in a GG-WT cell. The kymograph shows that a $[Ca^{2+}]_{fla}$ elevation directly precedes flagella lifting in the uppermost flagellum (f1). The trace below indicates that the $[Ca^{2+}]_{fla}$ elevation is restricted to the lifting flagellum only. Bar = 5 µm. **B**) Quantitation of $[Ca^{2+}]_{fla}$ elevations associated with flagella lifting in GG-WT and GG-IFT54-MS cells. The percentage of lifting events that coincide with a $[Ca^{2+}]_{fla}$ elevation is shown. **C)** Detailed examination of the timing of $Ca^{2+}$ signalling during flagella lifting in GG-IFT54-MS cells. The $[Ca^{2+}]_{fla}$ elevation (red) precedes the movement of the flagellum (shown by the position of the flagella tip – grey line) by 200 ms. Note that the increase in G-GECO fluorescence was not accompanied by any significant increase in the fluorescence of IFT54-mScarlet (blue line) indicating that changes in G-GECO fluorescence were not the result of movement artefacts. **D)** Kymograph indicating the response of a IFT54-MS cell to the removal of blue light. Movement and subsequent lifting of flagella caused by the removal of blue light (488 nm) is associated with removal of accumulations of paused retrograde IFT trains in the distal region. Bars = 5 µm and 15 s. **E**) Image series showing the response of IFT54-MS cell to the removal of blue light. The cells adopts the typical gliding configuration, with flagella arranged at 180˚ to each other, in the presence of blue light. . Removal of blue light at t = 0 s promotes withdrawal of flagella towards the cell body, so that only the flagella tips remain adherent. Bar = 5 µm. **F**) In the absence of external $Ca^{2+}$, the removal of blue light does not have any impact on accumulated IFT trains and flagella lifting did not occur. Bars = 5 µm and 15 s.

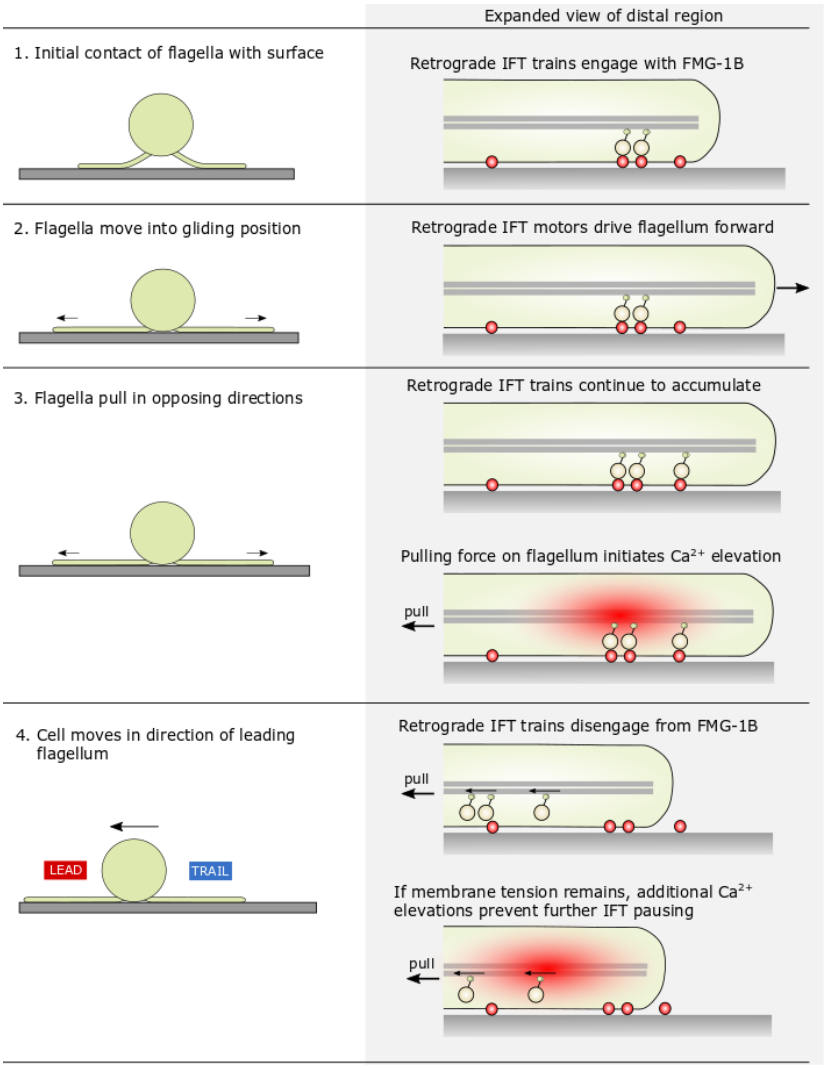


**Figure S7: Proposed scheme of the interaction between $Ca^{2+}$ and retrograde IFT trains.** 1) Following the initial contact of a flagellum with a surface, retrograde IFT trains begin to engage with adherent FMG-1B in the flagella membrane. 2) The accumulation of paused retrograde IFT trains pulls the flagellum forward (gliding motility) until both flagella are fully extended. The accumulation of paused retrograde IFT trains bound to FMG-1B means that the flagella resist pulling forces from the opposite direction. 3) If sufficient pulling force is applied, a mechanosensitive $Ca^{2+}$ elevation occurs in the flagellum, disrupting the interaction between FMG-1B and the paused retrograde IFT trains, causing the retrograde IFT trains to return to the cell body. 4) FMG-1B can therefore move freely in the flagella membrane, removing the resistance to the pulling force in this flagellum, which allows the flagellum to be dragged along the surface by the opposing flagellum.

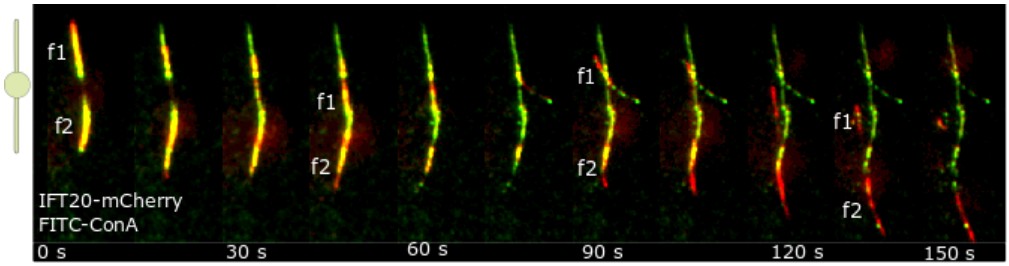


**Figure S8: Labelling of FMG-1B with fluorescent lectin.** Image series of gliding IFT20-mCherry (red) cell viewed by TIRF microscopy. The cell was labelled with the fluorescent lectin, fluorescein isothiocyanate- concanavalin A (FITC-ConA, green) prior to being allowed to settle. FITC-ConA labels the major adhesive glycoprotein, FMG-1B, in the flagella membrane. FMG-1B is shed from flagella during gliding and lifting movements, leaving behind a trail of the adhesive glycoprotein.

**Movie 1: $[Ca^{2+}]_{fla}$ elevations associated with movement in a gliding flagellum.**

TIRF microscopy of a GG-WT cell expressing CAH6-G-GECO. Significant $[Ca^{2+}]_{fla}$ elevations are associated with dragging movements in the flagellum, but $[Ca^{2+}]_{fla}$ elevations are not seen with forward movements in the flagellum.

**Movie 2: Repetitive $[Ca^{2+}]_{fla}$ elevations influence pausing of retrograde IFT.**

TIRF imaging of $[Ca^{2+}]_{fla}$ (G-GECO) in a flagellum on a 0.1% poly-lysine treated surface. In the initial period no $[Ca^{2+}]_{fla}$ elevations are observed. After 40 s a series of repetitive $[Ca^{2+}]_{fla}$ elevations are observed.

**Movie 3: Repetitive $[Ca^{2+}]_{fla}$ elevations influence pausing of retrograde IFT.**

TIRF imaging of IFT54-mScarlet in the flagellum shown in Video 2. In the initial period where no $[Ca^{2+}]_{fla}$ elevations were observed (Movie 2), IFT particles pause and accumulate in distal regions and very few retrograde IFT trains can be observed. After 40 s, when the series of repetitive $[Ca^{2+}]_{fla}$ elevations can be observed in Movie 2, the movement of IFT trains is noticeably different, with distinct retrograde IFT trains present.